Analyst

Proteomic and Direct Analysis in Real Time Mass Spectrometry Analysis of a Native American Ceremonial Hat

Journal:	*Analyst*
Manuscript ID	AN-ART-08-2019-001557.R1
Article Type:	Paper
Date Submitted by the Author:	10-Oct-2019
Complete List of Authors:	Cleland, Timothy; Smithsonian Institution, Museum Conservation Institute Newsome, G.; Smithsonian Institution, Museum Conservation Institute Hollinger, Eric; Smithsonian Institution, Anthropology Department, National Museum of Natural History

Proteomic and Direct Analysis in Real Time Mass Spectrometry Analysis of a Native American Ceremonial Hat

Timothy P. Cleland[1]*, G. Asher Newsome[1]*, R. Eric Hollinger[2]

*corresponding

[1]Smithsonian Institution, Museum Conservation Institute, Suitland, MD 20746

[2]Smithsonian Institution, National Museum of Natural History, Washington, DC 20560

Abstract

Complementary mass spectrometry analyses were performed to study a broken ceremonial hat of the Tlingit in the collection of the Smithsonian Institution National Museum of Natural History. The hat base and an associated cylinder are carved from wood and show multiple signs of age and breakage, as well as remnants of animal materials used for construction, decoration, and repair. Samples of animal tissues embedded in and attached to the wood were prepared for liquid chromatography-tandem mass spectrometry (LC-MS/MS), which identified proteins from five clades native to the object's area of origin. Surfaces on the hat and cylinder were analyzed using a direct analysis in real time (DART) MS system modified to accommodate the intact items. The presence of nicotine from tobacco smoke on the exterior and the relative absence of nicotine from the underside and formerly covered surfaces indicated that the cylinder was originally connected to the top of the hat. The characterization of the original object will be used to make informed decisions about reproduction of the intact hat for use by the Tlingit Kiks.adi clan.

Introduction

Cultural heritage objects provide critical information about past practices important to descendant communities for cultural preservation and perpetuation. However, little may be known of the methods or materials with which the objects were made, and analysis of the materials can provide a better understanding of past production processes. Mass spectrometry can provide a wealth of information about complex objects including species of origin of bio-organic tissues and the organic components that constitute paint or residues on the surface.

Previous studies using proteomics and liquid chromatography-tandem mass spectrometry (LC-MS/MS) used in museums, cultural heritage studies, etc. have resulted in more complete understanding of a variety of objects including the species of origin[1],[2],[3],[4]. For small molecule analysis, direct analysis in real time mass spectrometry (DART-MS) is increasingly popular for a wide variety of forensic applications[5] but is less commonly used specifically for analysis of historical materials. Several studies on historic textile dyes have been conducted with DART of fiber samples[6],[7],[8]. Mass spectrometry of objects using transmission mode DART generally requires a solid microsample to be dissolved[9],[10], made into a paste[11], or otherwise presented to the ion source in a form that can fit in the 1-2 cm between the probe and the inlet transfer tube. Ambient analysis of centrally located surface areas on intact objects without applying solvents requires operation in reflection mode.[12],[13] Complementary large and small molecule analyses provide a complete picture of an object.

Characterization of cultural heritage objects provides an opportunity to collaborate with indigenous communities to better understand their objects. The Smithsonian Institution has partnered with the Tlingit tribe of Alaska, USA, to analyze a broken ceremonial clan crest hat

collected in Sitka, Alaska, in 1884, using LC-MS/MS to identify animal tissue remnants and reflection mode DART-MS to characterize materials on the surface. The Tlingit Kiks.adi clan of Sitka asked the Smithsonian to digitize the hat, digitally repair the broken sections, utilize the digital model to mill a new replacement hat from wood, and paint and attach decorative materials to restore the hat. The chemical analysis of the original will be used to make informed decisions about the production of a replacement hat.

The sculpin hat and potlatch cylinder

The hat consists of a base in the form of a sculpin or bullhead fish (E74339) and a potlatch cylinder (E74441). The objects are in the collections of the Smithsonian Institution National Museum of Natural History (NMNH) and when collected in 1884 were noted to be "very old". A letter from the collector described the hat as a "large carved wooden helmet with wooden stove pipe attachment", but the 'attachment', or potlatch cylinder, had been separated during cataloging and was not recognized as related for the next 130 years. The hat and attachment were carved by an unknown artist from yellow cedar wood native to the Pacific Northwest, and each has multiple signs of repair and repainting from before they were collected. The round base hat is 46 cm in diameter and 20 cm tall, carved and painted with the form of the face of a sculpin or bullhead fish. A circular flat platform on top the head of the fish is hypothesized to be where the potlatch cylinder attached. The underside of the hat has an inner, carved rim the circumference of a human head. Sinew bands and a strip of commercial cloth are attached to the underside as a chinstrap. Fragments of various materials are embedded in the wood of the hat under paint and splinters, in pockets and holes, and under nail-heads. Both sides of the hat have been cracked and repaired with nails, lashings, and glue. Holes and square headed

nails in the platform on top of the hat show where an attachment was originally lashed to the broad base.

The cylinder is a single hollow log 56 cm long with a 15 cm diameter and is painted in stripes. It was split into two halves, carved out, and then lashed together. Age or stress has cracked the wood lengthwise, nearly separating it into more pieces. One end of the cylinder has nails embedded in the wood and a 3 cm wide coating of resin in which bits of hair and feathers are embedded.

Materials and Methods

Protein extraction and digestion

Eleven potentially proteinaceous samples (i.e., potential skin, leather, sinew) were taken from the sculpin hat and potlatch cylinder (Supplementary Figure 1). Subsamples of each sample (Table 1) were homogenized into 400 mM ammonium phosphate dibasic, 200 mM ammonium bicarbonate, 4 M guanidine hydrochloride using an Omni International Bead Ruptor Elite (45 s homogenization, 5 min at -20°C, repeated 4 times).[14] Assuming a similar composition across each individual sample, ends or loose areas of the samples were chosen to subsample. Following homogenization, all samples were incubated in the homogenization buffer for 72 hr at 37°C. Remaining solids were pelleted at 14,000 rcf for 10 minutes. Following incubation, protein concentration was measured using the Pierce BCA assay with bovine serum albumin as a protein standard.

Table 1: Masses of each potential skin, leather, sinew subsample used for protein extraction

NMNH E074441	
TL3	0.4 mg
TL8	2.4 mg
NMNH E074339	
TL6	0.1 mg
TL7	0.4 mg
TL12	0.4 mg
TL13	1.0 mg
TL14	2.5 mg
TL15	1.5 mg
TL17	0.7 mg
TL18	0.7 mg
TL19	3.3 mg

All extractions were treated the following way: proteins (15 µg, 14.4 µg for TL17) were buffer exchanged with 10,000 MWCO Milipore Microcon filters into 8 M urea (3x 10 min at 14,000 rcf) then reduced with 100 mM DTT at 65°C for 30 min. The proteins were then digested using a standard filter-aided sample preparation (FASP) method[15,16] on the same filters. Proteins were digested overnight with Promega modified trypsin (1:100) on the filter in a humidity chamber. Peptides were collected by centrifugation then desalted 3M Empore C18 stage tips.[17] All peptides were dried and re-suspended in 0.1% formic acid.

Nano-liquid Chromatography coupled to an LTQ Velos Orbitrap

Peptides (0.5 µg) were trapped on an in-house packed Thermo BioBasic C18 column (75 µm i.d., 5 µm particle size, 3 cm long) then separated on an in-house packed Thermo BioBasic C18 column (75 µm i.d., 5 µm particle size, 21 cm long). Peptides were separated on a gradient

from 2-55% B over 90 minutes. Buffer A was 0.1% formic acid and buffer B was 99.9% acetonitrile with 0.1% formic acid. Peptides were nanosprayed into a ThermoScientific LTQ Orbitrap Velos and analyzed with the following parameters: MS1: 60k resolving power, 100 ms ion time, 1E6 automatic gain control (AGC) target; MS^2: top 8 peaks fragmented with higher-energy collisional dissociation (HCD; 30% normalized collision energy [NCE]), 15k resolution, 5 *m/z* isolation width, 250 ms ion time, 5E5 AGC target. Prior to running samples, a cytochrome c peptide standard was injected two or more times.

Data Analysis

All sample and control RAW files were searched against a Mammalia (June 19, 2017) or Archosauria (August 28, 2017) database downloaded from Uniprot with PEAKS 8.5. Peptides were filtered at a 1% false discovery rate (FDR). Unique peptides detected by PEAKS were searched against the NCBI nr (non-redundant) protein database using the basic local alignment search tool (BLAST) to identify which taxa represented by the detected peptide sequences. Localization of post-translational modifications, and sequence variants with the same mass change, can change the interpretation of the species of origin. As a result of a combination of hydroxylation placement and mass shift between alanine and serine, one collagen III alpha 1 peptide was further interrogated with Prosight Lite (v1.4 Build 1.4.6) to evaluate the two modifications. The pattern of hydroxylation and amino acid sequence with the lowest probability score (P-score) was the most likely and retained here.

Ambient Surface Analysis

The LTQ Orbitrap Velos mass spectrometer was fitted with a differentially-pumped Vapur interface for analysis with a DART-100 probe in reflection mode operated by an SVP controller (IonSense, Saugus, MA). To accommodate surface sampling of large, intact objects, the standard 4-7 cm ceramic transfer tube to the Vapur interface was replaced with a 30 cm long, ¼" o.d. stainless steel tube at room temperature.[18] The tube was curved over the entire length, culminating with the orifice 45° to a horizontal sample surface (Supplemental Figure 2). To maximize DART probe clearance, all housing and heat shielding was removed from the flow cell. The DART probe was custom-mounted from above with multi-dimensional translation stages attached to the end of an adjustable Leica surgical microscope floor stand. The tip of the tapered ceramic insulator cap, also angled 45° to a sample surface, was positioned 2.5 mm in front of the transfer tube and 0.5 mm above the sample surface. An electronically-controlled shutter[13] was mounted above sample surfaces and beneath the ceramic cap and the transfer tube. Objects were supported from below and moved into position with a translatable platform on a tripod to analyze flat object surfaces and the tangent points of curved surfaces. To access an end of the cylinder, the artifact was positioned on the opposite end on top of lab jacks on the floor. DART analysis was performed at various helium temperature settings from 100 to 500 °C over 0.25 to 20 s shutter exposures. MS data was acquired at 30,000 resolving power with a maximum ion trap fill time of 100 ms.

Results and Discussion

Proteomic analysis

Sculpin hat (NMNH E074339)

Nine potentially proteinaceous samples were collected from the sculpin hat (TL6, TL7, TL12, TL13, TL14, TL15, TL17, and TL18). Two samples (TL6 and TL7) had no identifications (Table 2). Samples TL12, TL13, and TL15 were identified as mustelid (in context, most likely stoat/ermine) based on collagen I alpha 2 and collagen III alpha 1 peptides. TL14 was identified as *Haliaeetus leucocephalus* (bald eagle) based on collagen III alpha 1 and dermatopontin peptides. One collagen III alpha 1 peptide detected by PEAKS (GDSGAPGPKGETGLPGANGAPGQPGP*R) was re-examined by Prosight Lite to evaluate localization of hydroxylation on the peptide. With Prosight Lite, the revised peptide (GDSGAPGPKGETGLPGANGSPGQPGPR) was found to have a P-score of 1.3e-45 whereas the original peptide had a P-score of 4.9e-36 (Fig. 1).

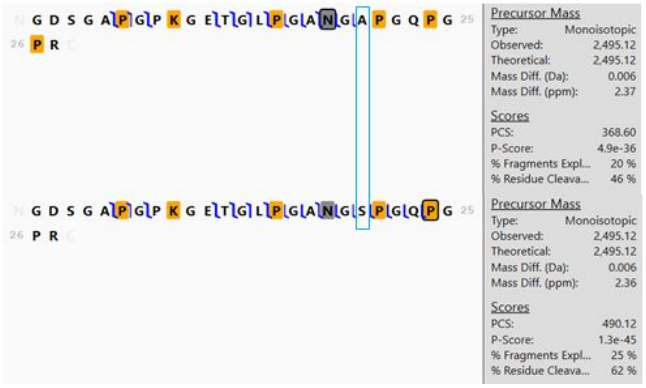

Figure 1: Prosight Lite characterization of collagen III alpha 1 peptide from *Haliaeetus leucocephalus.* Top: Original PEAKS identified peptide. Bottom: Revised peptide with Ala20->Ser20, Hyp26->Pro26. Higher PCS and lower P-Scores are better. Orange boxes are hydroxylation (+15.9949 Da), gray boxes are deamidation (+0.98402 Da), blue brackets represent b- and y- fragment ions, and light blue box between the sequences denotes the Ala20 -> Ser20 modification.

On the corrected peptide, Ala20 became Ser20 and Hyp26 became Pro26. The movement of hydroxylation from the X-position proline to serine better reflects the fragmentation pattern derived from the precursor peptide ion. This collagen III peptide was chosen because it is the sequence for *Haliaeetus* reflecting the taxonomically specific dermatopontin peptide. The

dermatopontin peptide suggests this sample is derived from bald eagle skin. We used Prosight Lite[19], a tool created for annotation of top down protein data, to evaluate the annotation/sequence of this collagen III peptide because it can quickly provide both fragmentation coverage and statistical metrics of quality without extended search time utilizing database searching. These statistical outputs allowed us to objectively evaluate the fragmentation, sequence, and PTM variation across this peptide. Bald eagle derived proteinaceous decorations are used extensively by the Tlingit[20] with these peptides likely deriving from skin. Sample TL17 was found to be derived from equid, sheep, or goat based on collagen I alpha 2 peptides. Unfortunately, the diagnostic peptide that can separate these taxa was not detected. TL18 was found to be cervid based on collagen I alpha 2 peptides. It is unclear which cervid species this sample is derived because local cervid species are not present within the database (e.g., moose, black deer, mule deer). TL19 was found to be walrus based on collagen III alpha 1 and collagen I alpha 2 peptides. Like the bald eagle skin, walrus derived materials have been used in Tlingit objects.[20]

Table 2. BLAST results for samples from the Sculpin hat (NMNH E074339).

Peptide	Sample Location	BLAST Top Match	BLAST Second Match	Protein
Sample TL6	Under nail head on back of hat	No clear result		
Sample TL7	Possible cordage from hole on upper back of hat	No clear result		
Sample TL12	**Contents of hole near edge of left brim**	**Mustelid**		
Collagen I alpha 2		HGNRGEPGPAGS VGPVGAAGPR	Mesocricetus auratus, **Enhydra lutris kenyoni, Mustela putorius furo**, Odobenus rosmarus divergens, Neomonachus schauinslandi, Leptonychotes weddellii	Oryctolagus cuniculus, Mus musculus, Rattus norvegicus, Mus caroli, Chrysochloris asiatica

Collagen I alpha 2		GEPGPAGSVGPV GAAGPR	Mesocricetus auratus, **Enhydra lutris kenyoni, Mustela putorius fur**o, Odobenus rosmarus divergens, Neomonachus schauinslandi, Leptonychotes weddellii	Oryctolagus cuniculus, Mus musculus, Rattus norvegicus, Mus caroli, Chrysochloris asiatica
Collagen I alpha 2		GFPGAPGNIGPA GK	**Enhydra lutris kenyoni, Mustela putorius furo**	Ursus maritimus, Panthera tigris altaica, Odobenus rosmarus divergens, Felis catus, Ailuropoda melanoleuca, others
Collagen III alpha 1		GPPGAVGPAGPR	Ursus maritimus, **Mustela putorius furo,** Odobenus rosmarus divergens, Camelus ferus, Camelus bactrianus, Camelus dromedarius, Leptonychotes weddellii	Sus scrofa, Ailuropoda melanoleuca, Ailuropoda melanoleuca, Galeopterus variegatus, **Enhydra lutris kenyoni**
Sample TL13	**Knotted cordage from hole near back edge**	**Mustelid**		
Collagen I alpha 2		GFPGAPGNIGPA GK	Enhydra lutris kenyoni, Mustela putorius furo	Ursus maritimus, Panthera tigris altaica, Odobenus rosmarus divergens, Felis catus, Ailuropoda melanoleuca, others
Sample TL14	**Contents of hole from on left side 6 cm from edge**	**Sea Eagle (Bald eagle)**		
Collagen III alpha 1		GDSGAPGPKGET GLPGANG**S**PGQP G**P**R (PEAKS detected GDSGAPGPKGET GLPGANGAPGQP GPR) Using Prosight Lite corrected to Ala20->Ser20 and Hyp26->Pro26 (Corrected P-score: 1.3e-45, Original P-score 4.9e-36)	Apteryx australis mantelli, Chaetura pelagica, Struthio camelus australis, Anser cygnoides domesticus, Aquila chrysaetos canadensis, Nipponia nippon, **Haliaeetus leucocephalus,** Gavia stellata, Pygoscelis adeliae, Aptenodytes forsteri, Eurypyga helias, Tinamus guttatus, Phaethon lepturus, **Haliaeetus leucocephalus,** Phalacrocorax carbo, Balearica regulorum	Picoides pubescens, Charadrius vociferus, Merops nubicus, Sturnus vulgaris, Calypte anna, others

			gibbericeps, Fulmarus glacialis	
Collagen III alpha 1/Collagen II alpha 1		GERGPPGETGPQGIVGGR	**Haliaeetus leucocephalus**, Phaethon lepturus, **Haliaeetus albicilla**	Aquila chrysaetos canadensis, Gavia stellata, Eurypyga helias,
Collagen III alpha 1/Collagen II alpha 2		GESGSPGPPGPPGHPGPAGSNGAPGK	**Haliaeetus leucocephalus**, Phaethon lepturus, **Haliaeetus albicilla**	Apteryx australis mantelli, Aquila chrysaetos canadensis, Colius striatus, Gavia stellata, Pygoscelis adeliae, Aptenodytes forsteri, others
Dermatopontin		GATTTFSAVNR	**Haliaeetus albicilla, Haliaeetus leucocephalus**	Ailuropoda melanoleuca, Chelonia mydas, Ursus maritimus, Pelodiscus sinensis, Leptosomus discolor, Merops nubicus
Sample TL15	**Contents of hole near front broken edge of rim**	**Mustelid**		
Collagen I alpha 2		GFPGAPGNIGPAGK	Enhydra lutris kenyoni, Mustela putorius furo	Ursus maritimus, Panthera tigris altaica, Odobenus rosmarus divergens, Felis catus, Ailuropoda melanoleuca, others
Sample TL17	**Contents of painted-over hole near right edge of rim**	**Equid or Sheep or Goat**		

Collagen I alpha 2		GYPGNAGPVGAAGAPGPQGPVGPTGK	Capra hircus, Ovis aries	Odocoileus virginianus texanus, Cervus elephas hippelaphus, Bos indicus, Pantholops hodgsonii, bos mutus, Bos taurus, Oryctolagus cuniculus, Bubalus bubalis, Equus caballus, Equus asinus, others
Collagen I alpha 2		GAPGAVGAPGPAGANGDRGEAGAAGPAGPAGPR	Equus asinus, Equus caballus	Homo sapiens, Tursiops truncatus, Orcinus orca, Bubalus bubalis, Odocoileus virginiaus texanus, Capra hircus, Pantholops hodgsonii, Ovis aries, others
Sample TL18	**Knotted sinew from right underside of hat**	**Cervid**		
Collagen I alpha 2		GEPGPAGAVGPAGAVGPR	Bos mutus, **Odocoileus virginianus texanus**, Bos indicus, Bos taurus, Bubalus bubalis, Bos mutus, **Cervus elaphus hippelaphus**	Cricetulus griseus, Elephantulus edwardii, Microtus ochrogaster, Sus scrofa domesticus, Miniopterus natalensis, Ursus maritimus, Ailuropoda melanoleuca
Collagen I alpha 2		GETGLRGDIGSPGR	Bos mutus, **Odocoileus virginianus texanus**, Bos indicus, Bos taurus, Bubalus bubalis, Bos mutus, Cervus elaphus hippelaphus	
Sample TL19	**Sinew from left underside ear loop connecting to chin strap**	**Walrus**		
Collagen III alpha 1		GPPGAVGPAGPR	Ursus maritimus, Mustela putorius furo**, Odobenus rosmarus divergens**, Camelus ferus, Camelus bactrianus, Camelus dromedarius, Leptonychotes weddellii	Sus scrofa, Ailuropoda melanoleuca, Galeopterus variegatus, Enhydra lutris kenyoni

Collagen III alpha 1		GDSGAPGERGPP GAVGPAGPR	Ursus maritimus, Mustela putorius furo, **Odobenus rosmarus divergens**, Leptonychotes weddellii	Sus scrofa, Camelus ferus, Camelus bactrianus, Camelus dromedarius, Ailuropoda melanoleuca, Enhydra lutris kenyoni, others
Collagen I alpha 2		GFPGAPGNVGPA GK	Ursus maritimus, Panthera tigris altaica, **Odobenus rosmarus divergens**, Felis Catus, Ailuropoda melanoleuca, Hipposideros armiger, Canis lupus familiaris, Neomonachus schauinslandi, Leptonychotes weddellii, Panthera pardus	Enhydra lutris kenyoni, Mustela putorius furo, Rhinolophus sinicus, Pteropus alecto, Eptescicus fuscus, Erinaceus europaeus, others
Collagen III alpha 1		DSGAPGERGPPG AVGPAGPR	Ursus maritimus, Mustela putorius furo, **Odobenus rosmarus divergens**, Leptonychotes weddellii	Sus scrofa, Camelus ferus, Camelus bactrianus, Camelus dromedarius, Ailuropoda melanoleuca, Enhydra lutris kenyoni, others
Collagen I alpha 2		GEPGPAGSVGPV GAAGPR	Mesocricetus auratus, Enhydra lutris kenyoni, Mustela putorius furo, **Odobenus rosmarus divergens**, Neomonachus schauinslandi, Leptonychotes weddellii	Oryctolagus cuniculus, Mus musculus, Rattus norvegicus, Mus caroli, Chrysochloris asiatica

Potlatch cylinder (NMNH E074441)

Two proteinaceous samples were collected from the potlatch cylinder (TL3 and TL8). Identified peptides were BLAST searched to identify their possible taxon of origin combining multiple peptides when possible. TL3 was determined to be mustelid (Table 3) based on peptides from collagen I alpha 2 and collagen VI alpha 1. TL8 was determined to be walrus in origin based on a combination of collagen I alpha 2 and collagen III alpha 1 peptides. Many overlapping taxa (e.g., *Ursus maritumus*) were detected for one of the collagen I alpha 2 and

collagen III peptides, but a second collagen I alpha 2 peptide eliminated *Ursus* from being a possibility. Based on the results from these samples, collagen III is more species specific than collagen I. More examination of sequence homology is necessary to evaluate the variation of collagen III sequence.

Table 3: BLAST search results from the potlatch cylinder (NMNH E074441)

Protein	Sample Location	Peptide	BLAST Top Match	BLAST Second Match
Sample TL3	**Leather under nail head at end of cylinder**	**Mustelid**		
Collagen I alpha 2		GFPGAPGNIGPAGK	Enhydra lutris kenyoni, Mustela putorius furo	Ursus maritimus, Panthera tigris altaica, Odobenus rosmarus divergens, Felis catus, Ailuropoda melanoleuca, others
Collagen VI alpha 1		WLAGGTFTGEALQYTR	Monodelphis domestica, Mustela putorius furo	Saimiri boliviensis boliviensis, Pongo abelii, Phascolarctos cinereus, Nomascus leucogenys, others
Sample TL8	**Raw hide loop holding two halves of cylinder together**	**Walrus**		
Collagen I alpha 2		GFPGAPGNVGPAGK	Ursus maritimus, Panthera tigris altaica, **Odobenus rosmarus divergens**, Felis Catus, Ailuropoda melanoleuca, Hipposideros armiger, Canis lupus familiaris, Neomonachus	Enhydra lutris kenyoni, Mustela putorius furo, Rhinolophus sinicus, Pteropus alecto, Eptescicus fuscus, Erinaceus

			schauinslandi, Leptonychotes weddellii, Panthera pardus	europaeus, others
Collagen III alpha 1		GDSGAPGERGPPGAVGPAGPR	Ursus maritimus, Mustela putorius furo, **Odobenus rosmarus divergens**, Leptonychotes weddellii	Sus scrofa, Camelus ferus, Camelus bactrianus, Camelus dromedarius, Ailuropoda melanoleuca, Enhydra lutris kenyoni, others
Collagen I alpha 2		GEPGPAGSVGPVGAAGPR	Mesocricetus auratus, Enhydra lutris kenyoni, Mustela putorius furo, **Odobenus rosmarus divergens**, Neomonachus schauinslandi, Leptonychotes weddellii	Oryctolagus cuniculus, Mus musculus, Rattus norvegicus, Mus caroli, Chrysochloris asiatica

Database searching for detecting unexpected taxa

All data were initially searched against the Mammalia database, but as described above, one of the samples was derived from *Haliaeetus*. When this sample was searched against Mammalia few identifications (1828 PSMs at 1% FDR) were made despite abundant MS2 spectra. We subsequently searched the same raw data against an Archosauria database and found abundant peptides (4401 PSMs at 1% FDR) to multiple bird species. Based on this case study, search strategies that utilize multiple independent databases is effective at finding unexpected results as well as the sensitivity to not have false discovery of species. The relatively small databases (compared to all of Uniprot or NCBI) retains the strong statistical identifications while still detecting species from multiple groups.

Ambient surface analysis

To assess potential damage to the hat and cylinder artifacts from DART analysis, a plank of acrylic-painted and unpainted yellow cedar wood was exposed to the DART gas plume for varying times at different temperature settings (Supplemental Figure 3). Thermal scorch marks on unpainted wood and on sections with white acrylic paint were observed after 20 s exposures to DART with helium temperature settings of 400 °C or higher. Artifact analyses were subsequently performed for 3 s with helium temperature settings of 300 °C to prevent damage.

Nine discrete surfaces (Supplementary Figure 4) on the carved hat were analyzed by DART after positioning the object in various positions beneath the DART ceramic cap, shutter, and transfer tube (Figure 2a, b). The potlatch cylinder was similarly analyzed on six discrete external surfaces, on the ~1 cm wide interior surface of a lengthwise crack, and on a nail head protruding from one end (Figure 2c). To access the narrow crack interior, the DART flow cell had to be positioned close to the greater external body of the cylinder. To prevent inadvertent heat exposure to the artifact and thermal desorption of analyte into the background, the adjacent cylinder body was covered with aluminum foil for the duration of the analysis (Figure 2d).

Figure 2. Reflection mode DART sampling configurations with extended transfer tube and shutter for selected surfaces on hat (a, b) and cylinder (c, d).

The chemical formulae were determined for 111 ions observed from at least one of 18 wooden surfaces sampled on the yellow cedar plank, hat, and cylinder. Flat surfaces tended to produce higher absolute signal intensity than the tangent of curved surfaces because of better flow dynamics in reflection mode. The surface of one end of the potlatch cylinder coated with resin produced the highest signal intensity from the ease of thermal desorption. Most observed ions had the form of protonated molecules ($[M + H]^+$) or fragments of protonated molecules, and some analytes also had ammoniated ($[M + NH_4]^+$) analogues from reaction with trace ammonia that is typically present in the ambient atmosphere. Example mass spectra from the hat and cylinder are shown in Supplemental Figure 5. The presence or absence of a particular ion in the DART mass spectrum of each of the various surfaces tested on the hat is listed in Supplemental Table 1, and surfaces on the cylinder and test plank are listed in Supplemental Table 2. Many compounds were observed on most surfaces, but only five compounds were observed on every wooden surface tested from all three objects: $C_{11}H_{11}NO$, $C_{17}H_{25}N$, $C_{17}H_{23}NO$, $C_{17}H_{25}NO$, and $C_{17}H_{23}NO_2$.

Various surfaces were differentiated by marker compounds. $C_{23}H_{48}N_2O$, *m/z* 369.3850, was observed exclusively from the two red surfaces tested on the hat. $C_{24}H_{35}N_5O_7$, *m/z* 506.2613, was observed exclusively from all surfaces on the hat and not the cylinder; $C_{30}H_{45}NO_5$, *m/z* 500.3381, was observed exclusively from the rim of the cylinder. Although the sinew stitching on the hat could not be sampled completely independently from the wood, two compounds were identified exclusive to the sinew: $C_8H_{14}O_4$ and $C_9H_{16}O_4$. Almost no analyte signal was observed from the nail head, except cholesterols from human handling and eugenol.

Nicotine ($C_{10}H_{14}N_2$) was observed at various levels on different surfaces of the hat and cylinder, which in the historical context of the objects is an unambiguous marker of tobacco smoke. To perform semi-quantitative analysis without applying an external chemical standard to the artifacts or undergoing further DART exposures, nicotine signal was compared to the summed signal of the five compounds observed on all surfaces ($C_{11}H_{11}NO$, $C_{17}H_{25}N$, $C_{17}H_{23}NO$, $C_{17}H_{25}NO$, and $C_{17}H_{23}NO_2$) as internal standards. Non-zero nicotine relative abundance was rated low or high, "high" nicotine levels being at least three times greater than "low" nicotine levels (Figure 3). The relative abundance of nicotine on the objects demonstrates how they were formerly connected and stored while exposed to smoke from tobacco, which the Tlingit are known to have used.[21] Nicotine levels were high on all external surfaces of the hat except the central flat top, suggesting that a covering, most likely the cylinder, had been attached to the top of the hat during the period of maximum exposure before the objects became disconnected. No nicotine was observed from the underside rim on which the hat rests stored. Similarly, high levels of nicotine were also observed on all external wooden surfaces of the cylinder. Low levels of nicotine were observed on the face of the fissure, indicating that primary tobacco smoke exposure occurred before the object cracked from age. The low but non-zero amount of nicotine on more recently exposed surfaces, i.e. the flat top of the hat and the cylinder crack interior, may have come from tobacco smoke exposure over the decades between the object accessioning and the ban on smoking in the museum. No nicotine was observed on the resin-coated surface of the cylinder, indicating that the resin was applied or re-applied to the wood after exposure to tobacco smoke. Combined with the fact that the cylinder and hat were never articulated in the museum, this suggests the majority of the nicotine exposure occurred while in use by the Tlingit, possibly in ceremony.

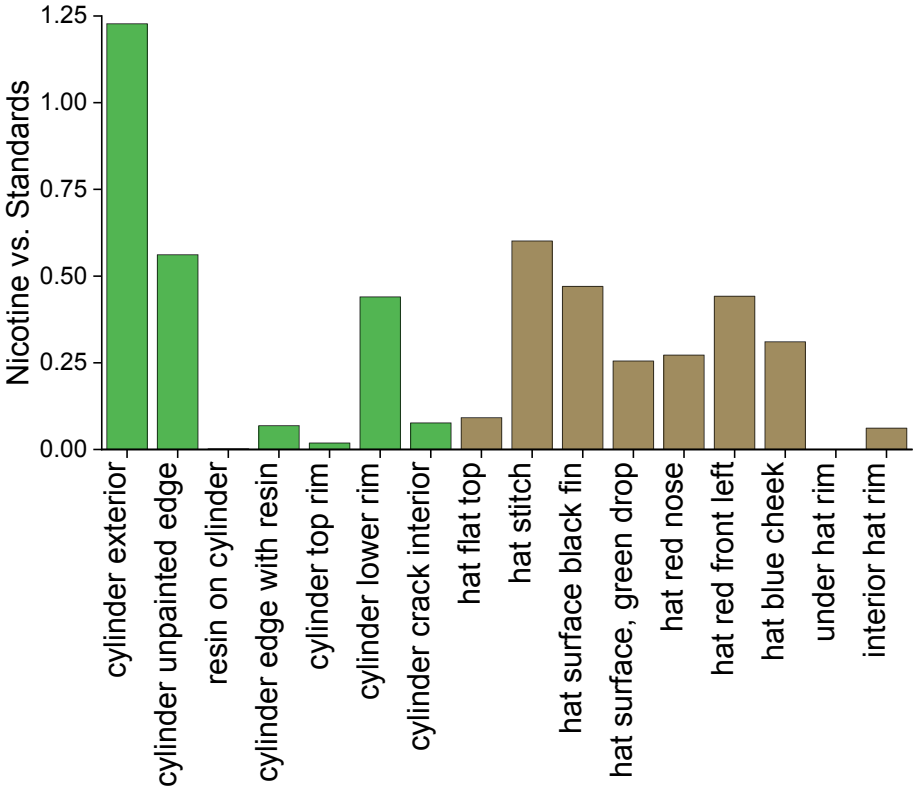

Figure 3. Ratio of nicotine signal abundance to standards for different surfaces of cylinder (green) and hat base (brown).

Acridine ($C_{13}H_9N$) is an N-heterocyclic polyaromatic hydrocarbon that has been identified from burning plant material[22] but has not been specifically associated with tobacco. Acridine signal was observed from DART analysis of the hat and cylinder and like nicotine was plotted relative to the summed abundance of the five marker ions (Figure 4). Acridine was observed on external surfaces in relative abundance similar to nicotine, but the higher signal of acridine on the flat top of the hat shows that the pieces were exposed differently to tobacco and wood smoke. Tlingit clan houses were large communal structures with openings only at the door and a central smoke hole, and wood smoke from fires used for light, heating, and cooking would

have been a common source of acridine. Because there was no source of secondary exposure to wood smoke, no acridine was observed in the cylinder fissure.

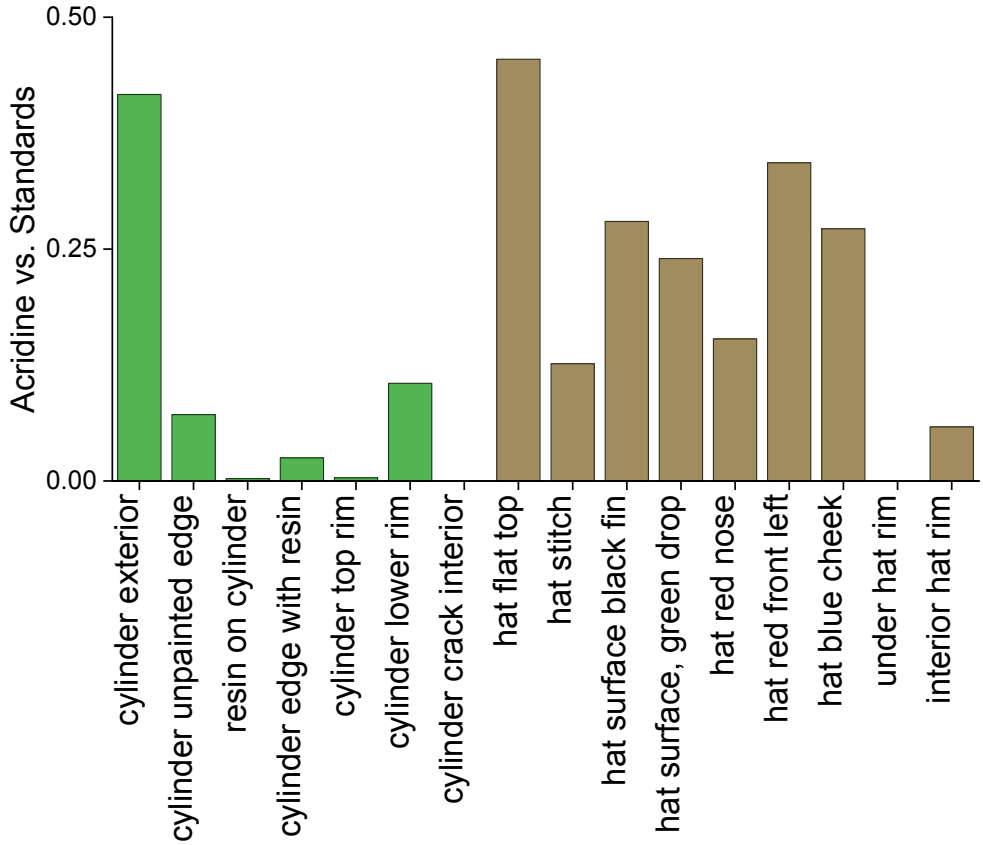

Figure 4. Ratio of acridine signal abundance to standards for different surfaces of cylinder (green) and hat (brown).

Conclusions

Proteomics has enabled identification of a large number of taxonomic origins for tissues attached to the sculpin hat and potlatch cylinders including unexpected origins of walrus and eagle. The presence of ermine, goat, deer, or elk was consistent with the species historically and

currently used for materials for regalia. Identification of these species gives a better understanding of how the wooden hat was originally adorned, guiding interpretations of how it was constructed and modified over its use life. These results were utilized by the Kiks.adi clan to decide what materials to use and how to attach them in a reproduction of the hat made in collaboration with the museum, which will serve the clan in ceremony in the future. The very small subsamples allow for future investigation of these same samples using other non-mass spectrometry techniques and reduces future need for destructive sampling from this cultural heritage object.

Reflection mode DART analysis of various surfaces on the sculpin hat and cylinder identified many organic compounds, some specific to one object or the other, to a paint, or to particular locations on the objects. The relative abundance of nicotine on various surfaces compared to internal standards (and differences from acridine) verified the former connectivity of the cylinder to the flat top of the hat before the objects were collected, and absence of signal from nicotine and acridine showed that the major tobacco and wood smoke exposure occurred before the cylinder was old enough to crack.

Acknowledgements

We would like to thank the Tlingit Kiks.adi clan and clan leader *Aanyaanax* (Ray Wilson, Sr.) for allowing us to collaborate in analyzing the sculpin hat and potlatch cylinder. We would also like to thank the Smithsonian Institution for funding. The NMNH Repatriation Office is grateful to the Smithsonian Women's Committee for funding the hat replication work which was supported by these analyses. All raw LC-MS and DART as well as PEAKS searches are

available on the MassIVE database at ftp://massive.ucsd.edu/MSV000084203/ (Reviewer access: ftp://MSV000084203@massive.ucsd.edu Username: MSV000084203 Password: Scu1p1n2019*)

References

1. M. D. Teasdale, S. Fiddyment, J. Vnoucek, V. Mattiangeli, C. Speller, A. Binois, M. Carver, C. Dand, T. P. Newfield, C. C. Webb, D. G. Bradley and M. J. Collins, *Royal Society Open Science*, 2017, **4**.
2. M. Mackie, P. Ruther, D. Samodova, F. Di Gianvincenzo, C. Granzotto, D. Lyon, D. A. Peggie, H. Howard, L. Harrison, L. J. Jensen, J. V. Olsen and E. Cappellini, *Angewandte Chemie-International Edition*, 2018, **57**, 7369-7374.
3. C. Solazzo, W. Fitzhugh, S. Kaplan, C. Potter and J. M. Dyer, *Plos One*, 2017, **12**.
4. A. K. Popowich, T. P. Cleland and C. Solazzo, *Journal of Cultural Heritage*, 2018, **33**, 10-17.
5. M. J. Pavlovich, B. Musselman and A. B. Hall, *Mass Spectrometry Reviews*, 2018, **37**, 171-187.
6. C. S. Deroo and R. A. Armitage, *Analytical Chemistry*, 2011, **83**, 6924-6928.
7. A. Kramell, F. Porbeck, R. Kluge, A. Wiesner and R. Csuk, *Journal of Mass Spectrometry*, 2015, **50**, 1039-1043.
8. R. A. Armitage, C. Day and K. A. Jakes, *STAR: Science & Technology of Archaeological Research*, 2015, **1**, 1-10.
9. J. Hopkins and R. A. Armitage, 2012.
10. D. Fraser, C. S. DeRoo, R. B. Cody and R. A. Armitage, *Analyst*, 2013, **138**, 4470-4474.
11. S. A. Torres, *McNair Scholars Research Journal*, 2014, **7**, 11.
12. T. T. Habe and G. E. Morlock, *Rapid Communications in Mass Spectrometry*, 2015, **29**, 474-484.
13. G. A. Newsome, I. Kayama and S. A. Brogdon-Grantham, *Analytical Methods*, 2018, **10**, 1038-1045.
14. T. P. Cleland and D. Vashishth, *Analytical Biochemistry*, 2015, **472**, 62-66.
15. J. Lipecka, C. Chhuon, M. Bourderioux, M. A. Bessard, P. van Endert, A. Edelman and I. C. Guerrera, *Proteomics*, 2016, **16**, 1852-1857.
16. J. R. Wiśniewski, A. Zougman, N. Nagaraj and M. Mann, *Nature methods*, 2009, **6**, 359.
17. J. Rappsilber, M. Mann and Y. Ishihama, *Nature Protocols*, 2007, **2**, 1896-1906.
18. A. Alvarez-Martin, T. P. Cleland, G. M. Kavich, K. Janssens and G. A. Newsome, *Analytical Chemistry*, 2019.
19. R. T. Fellers, J. B. Greer, B. P. Early, X. Yu, R. D. LeDuc, N. L. Kelleher and P. M. Thomas, *Proteomics*, 2015, **15**, 1235-1238.
20. Emmons, G. T.; De Laguna, F., The Tlingit Indians. University of Washington Press; American Museum of Natural History: Seattle New York, 1991; p xl, 488 p.
21. https://alaska.si.edu/record.asp?id=484, (accessed October 2019).
22. L. T. Fleming, P. Lin, A. Laskin, J. Laskin, R. Weltman, R. D. Edwards, N. K. Arora, A. Yadav, S. Meinardi, D. R. Blake, A. Pillarisetti, K. R. Smith and S. A. Nizkorodov, *Atmospheric Chemistry and Physics*, 2018, **18**, 2461-2480.